Chemical Engineering Science 121 (2015) 16–22

Contents lists available at ScienceDirect

Chemical Engineering Science

journal homepage: www.elsevier.com/locate/ces

Substrate directed self-assembly of anisotropic nanoparticles

Tarak K Patra, Parul Katiyar, Jayant K Singh *

Department of Chemical Engineering, Indian Institute of Technology Kanpur, Kanpur 208016, India

HIGHLIGHTS

- Molecular dynamics study on the self-assembly of anisotropic nanoparticles on a flat surface.
- Anisotropic particles induce directionality in the assembly process.
- Aggregation of anisotropic particles depends on their shape and size.
- A flat surface can drive linear aggregation of adsorbed tetrahedrons.
- Phase diagrams of tetrahedrons and triangles on a surface are presented.

ARTICLE INFO

Article history:
Received 29 April 2014
Received in revised form
10 September 2014
Accepted 13 September 2014
Available online 28 September 2014

Keywords:
Anisotropic nanoparticle
Self-assembly
Disorder–order transition
Aggregation
Coarse-grained simulation

ABSTRACT

We present a molecular dynamics study on the self-assembly of anisotropic nanoparticles—triangles and tetrahedrons on a flat surface. We observe ordered and disordered aggregates of nanoparticles depending on the particle–particle and surface–particle interactions. Anisotropic particles induce directionality in the assembly process. In particular, a cross over from the isotropic (spherical) assembly to the anisotropic (non-spherical) assembly of nanoparticles is identified as their size increases for weak nanoparticle–surface interactions. However, at strong nanoparticle–surface interactions, clusters of nanoparticles grow uniformly on the surface. We present phase diagrams that depict all possible structures of triangles and tetrahedrons depending on their size (L) and the nanoparticle–surface interaction strength (ε_{ns}). We show a disorder to order transition in the $L-\varepsilon_{ns}$ plane, as L and ε_{ns} increase.

1. Introduction

A remarkable variety of anisotropic colloidal nanoparticles (NPs)—cubes, rods, tetrahedrons, plates, tetrapods, octapods, bipyramids, janus particles, and many other shapes are synthesized in past few years (Glotzer and Solomon, 2007; Greyson et al., 2006; Ahmadi et al., 1996; Yamamuro et al., 2008). These particles have potential applications in photonics, energy storage devices, biological sensors, and many other micro/nanofluidic applications (Glotzer, 2004; Arciniegas et al., 2014; Stam et al., 2014). Vertically aligned nanopillers over a substrate, for example, is found to be a promising candidate for highly localized fluorescence imaging of single molecules (Xiea et al., 2011). Nanowires and nanotubes are used for building circuits in nanoscale electronics and optoelectronic devices (Duan et al., 2001). In addition, they find application in solar energy harvesting (Wanga et al., 2010), and are useful obstacles in nanodevices for separation of biomolecules (Seo et al., 2004). Similarly, optical, electrical, mechanical and catalytic properties of NPs of highly symmetric platonic shape, such as polyhedrons, could be tuned for specific applications (Kim et al., 2004; Millstone et al., 2009; Chan et al., 2008). Polyhedrons have preferred symmetry for 2D and 3D packing, which leads to many diverse structures and properties. Polyhedral shaped CdTe NPs, in a solution, self-assemble into a free floating sheet that displays considerable mechanical robustness (Tang et al., 2006). Further, polyhedral NPs show superior optical properties compared to spherical particles (Kasture et al., 2010). The optical properties of polyhedral gold nanoparticles also depend on their shape and size (Seo et al., 2008).

Therefore, the self-assembled structures of anisotropic particles have variety of interesting properties. In addition, certain viruses and other biological micro-organisms are of non-spherical geometry (Arkhipov et al., 2006). Hence, there is a growing research interest to study how the anisotropic particles interact among each other and with surfaces for understanding numerous biophysical processes and bio/nanotechnological applications (Li et al., 2011; Kinge et al., 2008;

* Corresponding author.
E-mail address: jayantks@iitk.ac.in (J. Singh).

http://dx.doi.org/10.1016/j.ces.2014.09.023
0009-2509/

Min et al., 2008; Grzelczak et al., 2010). The challenge is to assemble NPs into required structures to obtained desired properties. The ability to assemble NPs into a desired structure depends on the understanding and controlling of the inter-particle interaction (Bishop et al., 2009). Computer simulations can play an important role in the understanding of the inter-particle interaction of nanoparticles, and eventually predicting the phase behavior of NPs. Indeed, molecular simulations have revealed that the anisotropic interaction in bulk systems can lead to highly structural materials (Patra and Singh, 2014; Zhang et al., 2003; Zhang and Glotzer, 2004). However, the effects of surfaces/substrates on the structures of anisotropic particles are not well studied. A few examples have appeared where the assembly of NPs on a surface is greatly influenced by the structural details of the surface and the shape of NPs. For example, rod-like arrangements of gold NPs on a silicon surface are predominantly aligned along the principle crystallographic axis of the surface (Hayton et al., 2007). The asymmetrical van der Waal interaction is found as a powerful means to control orientation of multi-component cylindrical arrays on a stationary substrate (Smith et al., 2014). More complex structures form on non-stationary substrate such as membranes. For example, the equilibrium arrangement of rod-like NPs on a membrane is affected by the orientation-dependent interaction between them and dynamical traps caused by incorrect arrangements (Yue et al., 2013). Also, the wrapping of a non-spherical micro-organism on a cellular membrane is largely dependent on its aspect ratio (Dasgupta et al., 2014). Therefore, it is evident that the structural properties of nanoparticles on a substrate strongly influenced by their shape. In spite of few works on the behavior of anisotropic particles, mainly nanorods, on a surface, their aggregation mechanism is not well studied.

The objective of this study is to understand the aggregations of non-spherical particles on a surface, which are revealed in recent experiments (Bishop et al., 2009; Wang et al., 2007; Radha and Kulkarni, 2011). Experiments have shown that nanoparticles aggregate into varieties of superstructures (Ghezelbash et al., 2004). For example, pyramidal SnO_2 nanoparticles epitaxially grow on a surface of single crystalline ZnO nanobelts with different orientations (Wang et al., 2007). In addition, triangular microplates of Au self-organize into well-formed single crystalline triangles on a Si surface, and sometime plates are held vertically on the surface during the growth event (Radha and Kulkarni, 2011). Superstructures are very sensitive to the shape of nanoparticles. In a recent experiment study, Ming et al. have shown that Au nanorods, polyhedra, nanocubes and bipyramids aggregates into nematic/smetic-A, hexagonally packed, tetragonally packed, and nematic/3D ordered super structures, respectively (Ming et al., 2008). However, the growth mechanism is not well understood. Both anisotropic and isotropic growths are observed for non-spherical nanoparticles (Ahmadi et al., 1996; Kasture et al., 2010; Loudet et al., 2005; Camargo et al., 2010; Rycenga et al., 2008; Mu et al., 2012). In this work, we have studied the quantitative details of the inter-particle and surface–particle interactions that lead to the aggregation of non-spherical particles into larger isotropic or anisotropic structures. The packing of particles also depends on their shape (Li et al., 2011; Graaf et al., 2011; Damasceno et al., 2012; Henzie et al., 2012). Hard tetrahedrons are found to pack into pentagonal dipyramid, icosahedrons, nonamers and tetrahelixes depending on the applied pressure (Haji-Akbari et al., 2009). Tetrahedrons are usually packed in ordered structures in presence of an external field. However they spontaneously exhibit disorder and loose packing (Baker and Kudrolli, 2010). Thus, the aim of the current work is to study the self-assembly process of NPs and their packing on a flat substrate using molecular dynamics (MD) simulations. We have considered two different shapes namely tetrahedron and triangle in this study.

A NP contains hundred to millions of atoms depending on its size and chemical composition. The self-assembly of NPs is a slow process; therefore, it is computationally very expensive to perform all-atom simulations of the self-assembly of NPs on a surface. In the present study, we use coarse-grained models, in which group of atoms within a NP are replaced by a single coarse-grained bead, thereby presenting a larger scale description of the system.

The rest of the paper is organized as follows. The models of tetrahedron and triangle are presented along with the model of the substrate in Section 2. Section 2 also describes the simulation details. Results are presented and discussed in Section 3. Finally, the conclusions are drawn in Section 4.

2. Model and methods

We use coarse-grained models to represent triangle and tetrahedron. We construct a lattice structure according to the shape of a NP. A triangular lattice and an fcc lattice are used for triangular and tetrahedral NPs, respectively. Each lattice site represents a coarse-grained bead of a NP. The distance between two neighboring beads is σ. One NP is made of several frozen beads as shown in Fig. 1. The number of beads in a NP of edge length $L = l\sigma$ is given by $l(l+1)/2$ for triangle and $l(l+1)(l+2)/6$ for tetrahedron, where l is a positive integer. Our aim is to study the generic behavior of anisotropic nanoparticles, rather than a specific system. We, therefore, model the interaction between coarse-grained beads by an empirical pair potential. Any two beads from different NPs interact via the Lennard–Jones (LJ) potential,

$$V(r) = 4\varepsilon\left[\left(\frac{\sigma}{r}\right)^{12} - \left(\frac{\sigma}{r}\right)^{6}\right] - V(r_c). \quad (1)$$

Here, ε is the characteristic energy parameter. The pair potential represents dispersive and excluded volume interactions that are the characteristic of many NP systems (Patra and Singh, 2014; Zhang et al., 2003; Patra and Singh, 2013). We choose the cut-off distance $r_c = 2 \times 2^{1/6}\sigma$ to represent attractive interaction between NPs. The substrate is modeled as the (1 1 1) plane of an fcc lattice. Surface atoms are placed at lattice sites with neighbor distance of 1σ. The geometry of the flat surface is square. The system is periodic along the plane of the flat surface (xy-plane). Attractive surface–NP interactions are chosen to model adsorption of the NPs. NP beads and surface atoms interact through the LJ potential (cf. Eq. (1)) with the cut-off distance $r_c = 2 \times 2^{1/6}\sigma$. The interaction strength between the surface and NPs ε_{ns} is varied in this work. Surface atoms are also kept frozen in this work. The equations of motion are integrated with a time step of $0.01\tau_0$, where $\tau_0 = \sigma\sqrt{m/\varepsilon}$ is the unit of time and m is the mass of a bead of NPs. At each time step, frozen subunits of a NP move together as a rigid body using the method of quaternion (Miller et al., 2002). All the simulations are performed at a temperature $T = 1.0\varepsilon/k_B$, imposed using a Langevin thermostat (Zhang et al., 2003). Here, k_B is the Boltzmann constant. We have melted initial configurations at a

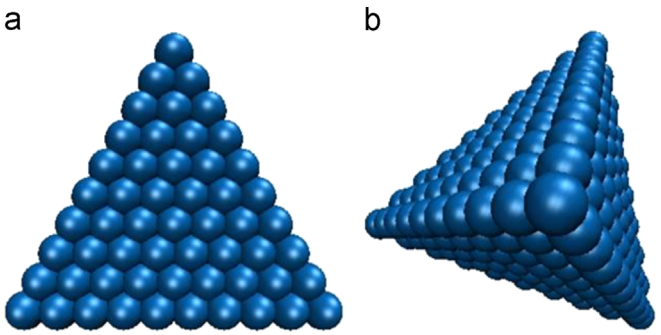

Fig. 1. Schematic representations of model NPs studied in this work: (a) triangle, and (b) tetrahedron.

very high temperature $T = 4.0\varepsilon/k_B$, followed by a slow temperature tunneling to the desired temperature. In the tunneling process, the temperature is gradually reduced by 0.2 unit after 10^6 MD time steps until it reaches $T = 1.0\varepsilon/k_B$. The systems are then equilibrated at the desired temperature for 2×10^8 steps followed by 10^7 production steps. Simulations are performed using the LAMMPS (Large-scale Atomic/Molecular Massively Parallel Simulator) package (Plimpton, 1995). All variables reported in this study are reduced by ε and σ.

3. Results and discussion

The self-assembly of NPs on the surface depends on their size, shape and interaction among themselves and with the surface. In this work, we have studied the effect of the size and shape of the NPs on their self-assembly behavior. First, we investigate the inter-particle interaction. Fig. 2 presents the pair interaction energy between two triangles as a function of the distance between them for different particle sizes (L). The pair interaction depends on the relative orientation between the two NPs. The interaction energy is shown for two different orientations—(i) face-to-face alignment i.e., the faces (planes) of two triangles are in parallel as shown in Fig. 2a, and (ii) edge-to-edge alignment i.e. the two edges (sides) of two different triangles are in parallel as shown in Fig. 2b. The well depth of the potential energy function is higher for the face-to-face alignment in comparison to the edge-to-edge alignment. As the size of the triangle increases, the well depth of the potential energy function increases. A significant difference in the well depth of the potential energy for two different alignments is observed for larger size particles. This indicates that the orientation of particles plays a crucial role in the assembly process of larger size particles. The potential energy as a function of inter-particle distance for tetrahedrons is shown in Fig. 3. Panels (a) and (b) correspond to face-to-face and edge-to-edge alignments of two tetrahedrons, respectively. The face-to-face alignment leads to deeper well depth in potential energy function, similar to that seen for triangles. For small size particles, the difference in the potential energy between the two orientations is not significant.

Now, we focus on the aggregations of nanoparticles on the surface. We simulate systems with number of NPs varying from 100 to 500 corresponding to a fixed loading. We define the loading as $\phi = (nN/L_s^2)$. Here, n, N and L_s correspond to the number of interaction sites (beads) in a NP, total number of NPs and length of the surface, respectively. We have considered $\phi = 0.3$. L_s is varied from 60 to 200 to maintain a particular loading. The triangular NPs aggregate into various super structures on the surface depending on their size and the surface–NP interaction. First we present a case

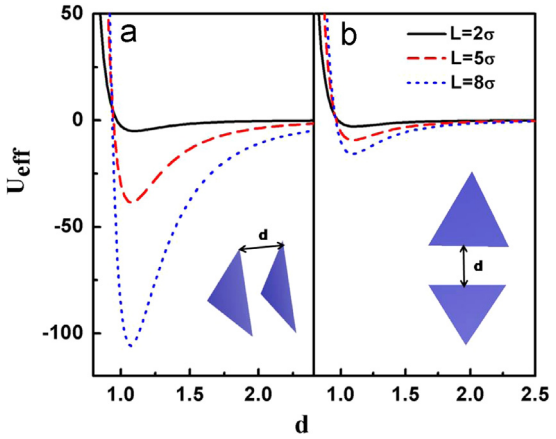

Fig. 2. The pair energy U_{eff} between two triangles, with different orientations, as a function of distance d between them. Panels (a) and (b) correspond to face-to-face and edge-to-edge alignments, respectively.

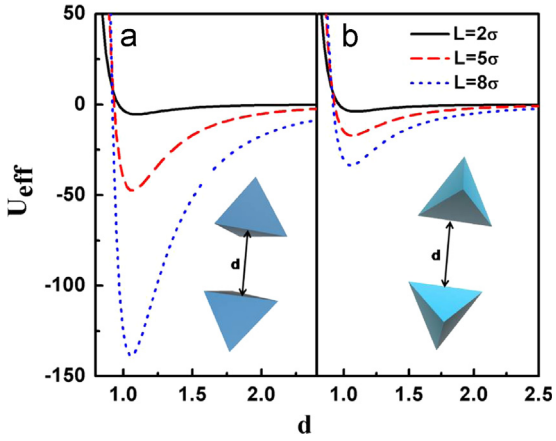

Fig. 3. The pair energy U_{eff} between two tetrahedrons, with different orientations, as a function of distance d between them. Panels (a) and (b) correspond to face-to-face and edge-to-edge alignments, respectively.

study for a weak surface–NP interaction strength $\varepsilon_{ns} = \varepsilon/2$. The MD snapshots of the aggregated structures of triangles are shown in Fig. 4. A semi-spherical disordered aggregate of triangles on the surface along with a gas-like phase is observed for $L=2$, as shown in Fig. 4a. In the disordered state, the particles aggregate without any crystal symmetry, and the cluster is amorphous in nature. As the particle size increases, the gas-like phase disappears, and we observe only disordered aggregates of triangles on the surface. For particle size $L \geq 4$, triangles align face-to-face and form stacks as shown in Fig. 4b–d. Stacks are aggregated into a super structure. They are aligned perpendicular as well as horizontal on the surface. For larger size particles, the growth of a cluster is anisotropic. For example, the cluster for $L=7$, as shown in Fig. 4d, is one-dimensional (1D) in nature. Similarly, disordered and ordered aggregates of tetrahedrons are formed on the surface depending on the particle size as shown in Fig. 5. For $L=2$, a disordered aggregate of NPs along with a gas-like phase form similar to the case of triangles. As L increases, ordered aggregations form. Interestingly, 1D string-like aggregates form for larger size particles such as for $L=5$ as shown in Fig. 5c. The structure in Fig. 5c is an interpenetrating pentagonal dipyramids. A unit of the structure i.e. a pentagonal dipyramid is shown separately in Fig. 5d, which consists of five tetrahedrons with face-to-face alignment.

The shape of a cluster varies depending on the size of individual particles in it. These are not even 2D aggregates, as expected for an attractive flat surface. The three dimensional (3D) growth (spherical clusters) is more pronounced for small size particles. In order to understand the cluster growth, we analyze the particle–particle and particle–surface interactions. Fig. 6a and b represent the NP–NP and NP–surface interaction energies E as a function of L for triangles and tetrahedrons, respectively. For a very small size ($L=2$) of NPs, NP–NP and NP–surface interaction energy are of the same order. As L increases, the NP–NP interaction energy falls sharply, and the NP–surface interaction energy decreases very slowly. For large size particles, the NP–NP interaction dominates over the NP–surface interaction, leading to the clusters growth perpendicular to the surface.

In order to understand the directionality of the self-assembly process and the shape of clusters, we have estimated the principal radii of gyration of clusters from their square radius of a gyration tensors. The square radius of gyration tensor of a cluster can be written as (Patra and Singh, 2014)

$$R^2_{\gamma\sigma} = \left[\frac{1}{N}\sum_{i=1}^{N}(\gamma_i - \gamma_{cm})(\beta_i - \beta_{cm})\right]. \quad (2)$$

Here, γ_i and β_i denote the position coordinates (x, y, and z) of the center of mass (CM) of a NP. γ_{cm} and β_{cm} are the coordinates of

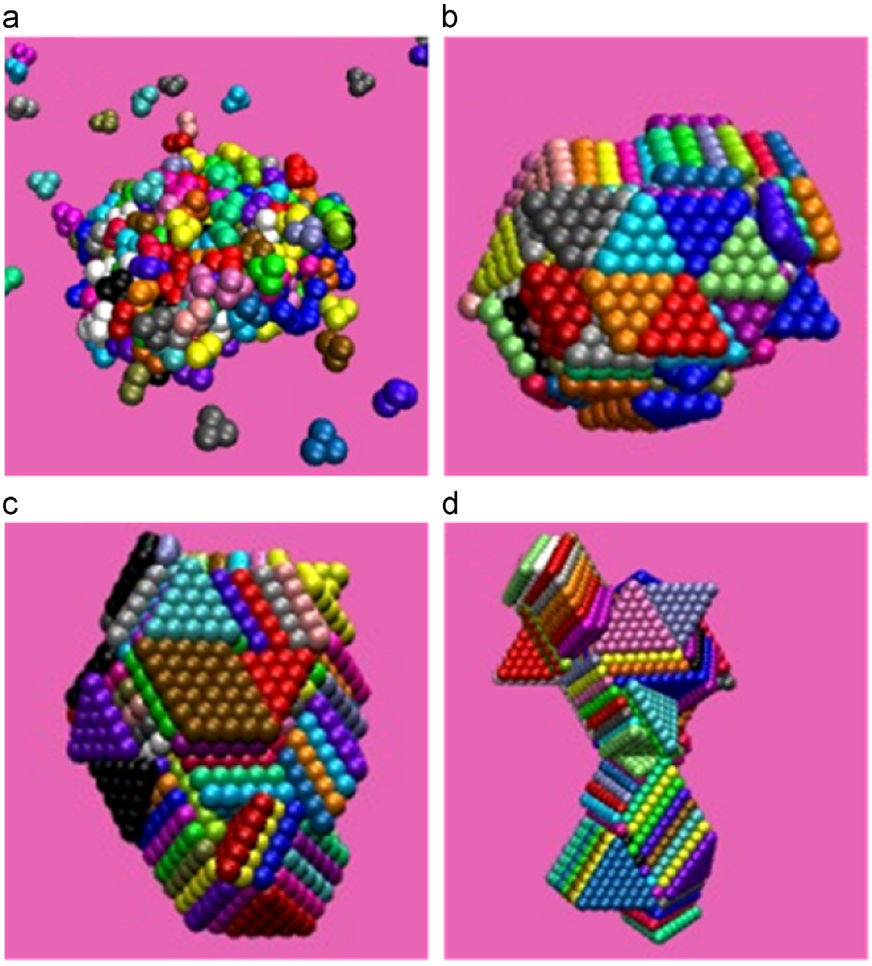

Fig. 4. MD snapshots of the clusters of triangles on the surface for $\varepsilon_{ns} = 0.5$, for (a) $L=2$, (b) $L=4$, (c) $L=5$ and (d) $L=7$.

the CM of a single cluster (x_{cm}, y_{cm}, and z_{cm}). N is the number of NPs present in a cluster. The Eigenvalues of the matrix are M_1, M_2, and M_3. Therefore, the three principal radii are $R_1 = \langle M_1 \rangle^{1/2}$, $R_2 = \langle M_2 \rangle^{1/2}$, and $R_3 = \langle M_3 \rangle^{1/2}$. R_1, R_2, and R_3 are identical for a perfect sphere (3D). In case of a 2D infinite sheet, one principal radius is finite, and the other two are infinite. On the other hand, two principal radii are equal and the third one is infinity for an infinitely long perfect cylinder (1D). The principal radii of gyration for a cluster of triangles are shown in Fig. 7a. The value of principal radii, R_1, R_2, and R_3 are of same order for $L \leq 4$. This indicates that the cluster is a spherical aggregate, as seen in the MD snapshot of Fig. 4b. Therefore, the growth of the cluster is isotropic for small size triangles. As the L increases beyond 4, the R_3 increases sharply. It is significantly higher than R_1 and R_2 for $L > 4$. This accounts for the 1D growth of the clusters, as L increases beyond 4. Similarly, Fig. 7b presents the principal radii of gyration for the cluster of tetrahedrons. R_1, R_2 and R_3 are of the same order for $L = 3$. This represents a spherical aggregate of tetrahedrons. As L increases, there are significant differences between the principal radii. For $L=4$, R_2 and R_3 are of comparable order, indicating a transition from 3D to 2D structure. Beyond $L=4$, R_3 is significantly higher than other two radii. This behavior indicates that the growth of the cluster of tetrahedrons is anisotropic (non-spherical or non-circular) when $L \geq 4$. In particular, the cluster grows one dimensionally for large size particles. The unusual behavior of R_3 is an indicative of a complex kinetic behavior (see Fig. 7a), which we plan to study in a future work.

Now, we focus on a case study where the NP–surface interaction strength is $\varepsilon_{ns} = \varepsilon$. As the NP–surface interaction is stronger, we observe in-plane growth of clusters. Figs. 8 and 9 represent the particle fraction perpendicular to the surface for triangles and tetrahedrons, respectively. The particles fraction is defined as $f(z) = n(z)/N$. Here, $n(z)$ is the number of particles at a distance z perpendicular to the surface, and N is the total number of particles in a system. The MD snapshots are shown in the inset of the figures. A distinct peak in $f(z)$ indicates a monolayer of triangles on the surface, as seen in Fig. 8a. The monolayer is disordered for $L=2$. However, an ordered monolayer is observed for $L=5$ as shown in Fig. 8b, where all the triangles have edge-to-edge alignment. In case of tetrahedrons, we also observe in-plane growth, as shown in Fig. 9. There are two distinguish peaks of $f(z)$ for $L=3$ as shown in Fig. 9a, indicating a bilayer. However, a monolayer is formed for $L=5$, which is represented by a single peak in Fig. 9b. The interaction energies between NP–NP and NP–surface are shown in Fig. 10a and b for triangles and tetrahedrons, respectively. The NP–surface interaction energy decreases faster than the NP–NP interaction energy. There are clear indications of the dominance of the NP–surface interaction as L increases. This is in contrast with the previous case of $\varepsilon_{ns} = \varepsilon/2$, where the NP–NP pair interaction dominates over the NP–surface interaction. In this work, we have studied the structural properties of the NPs for different values of the NP–surface interaction strength ε_{ns} ranging from 0.25 to 2.0, and L ranging from 2 to 8. Fig. 11 summarizes all possible arrangements of triangular NPs on the surface in a phase diagram. We observe disordered spherical aggregates of triangles for low values of ε_{ns} and L. As L increases, triangles align face-to-face and form ordered stacks for low ε_{ns}. The stacks are assembled into a non-spherical cluster. For a higher ε_{ns}, clusters grow uniformly on the surface, and

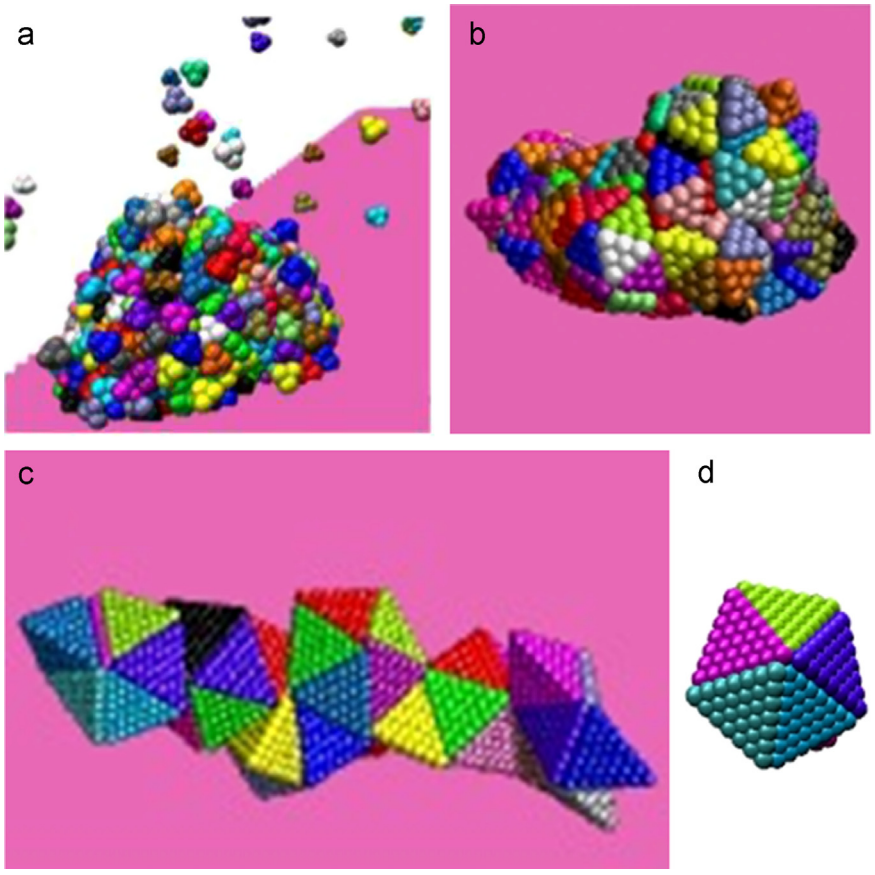

Fig. 5. MD snapshots of the clusters of tetrahedrons on the surface for $\varepsilon_{ns} = 0.5$, for (a) $L=2$ (side view), (b) $L=3$ and (c) $L=7$. Panel (d) represents a pentagonal dipyramid which is extracted from (c).

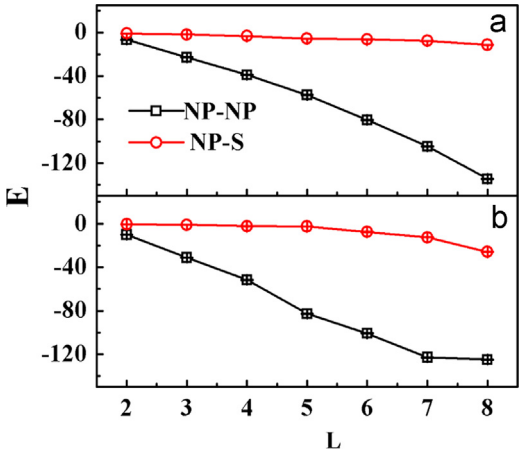

Fig. 6. NP-NP and NP-surface interaction energies of the system per NP (E) as a function of particle size (L) for $\varepsilon_{ns} = 0.5$, for (a) triangles and (b) tetrahedrons. Error bars are of the order of symbol sizes.

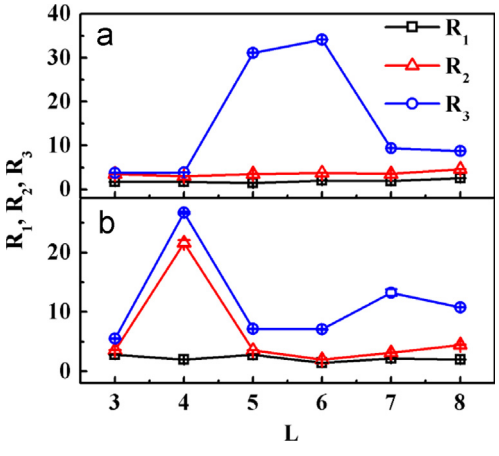

Fig. 7. The principal radii of gyration of the clusters as a function of particle size for $\varepsilon_{ns} = 0.5$, for (a) triangles and (b) tetrahedrons. Error bars are smaller than symbol size.

layers of triangles form on the surface. The layers are ordered except for $L=2$. Multilayers are seen for $\varepsilon_{ns} = 0.75$. As ε_{ns} increases further, only monolayers form. The phase diagram depicts an order to disorder transition in the $L-\varepsilon_{ns}$ plane. Fig. 12 presents the phase diagram for clusters of tetrahedrons on the surface. Similar to the previous case, the disorder to order transition is identified as L and ε_{ns} increase. In the non-spherical aggregates, which occur for large particle size ($L \geq 4$) and low NP–surface interaction ($\varepsilon_{ns} \leq 1.0$), tetrahedrons are aligned face-to-face, and the clusters consist of pentagonal dipyramids (cf. Fig. 5).

4. Conclusions

We have studied the structural properties of anisotropic particles—triangles and tetrahedrons on a flat surface using molecular dynamics simulations. We have used a coarse-grained model to delineate the generic behavior of triangles and tetrahedrons on the surface. This study has mainly focused on the effects of size, shape and NP–surface interaction strength on the self-assembly of NPs on a surface. We have calculated principal radii of gyration and interaction energies of clusters of NPs to analyze their structures

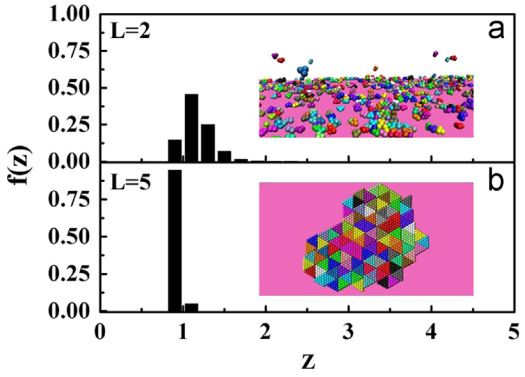

Fig. 8. Particle fraction profile normal to the surface for triangles, for (a) $L=2$ and (b) $L=5$. Corresponding MD snapshots are shown in the insets.

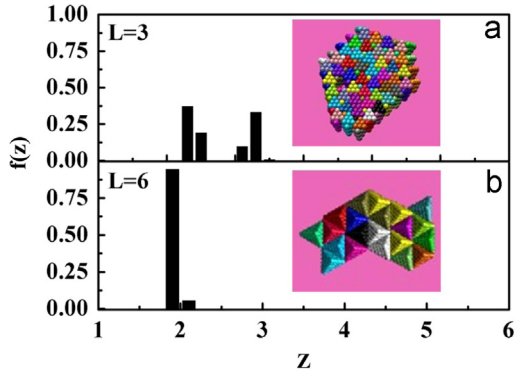

Fig. 9. Particle fraction profile normal to the surface for tetrahedrons, for (a) $L=3$ and (b) $L=6$. Corresponding MD snapshots are shown in the insets.

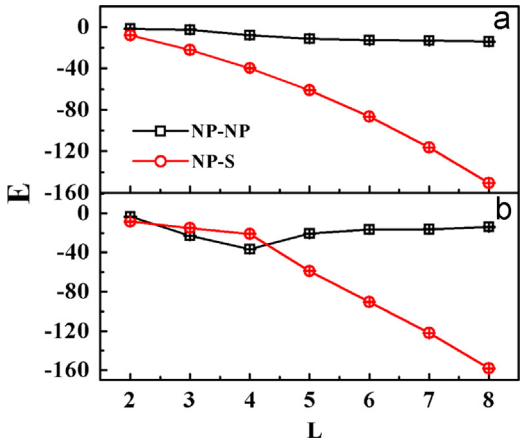

Fig. 10. NP-NP and NP-surface interaction energies of the system per NP (E) as a function of particle size (L) for $\varepsilon_{ns}=1.0$, for (a) triangles and (b) tetrahedrons. Error bars are of the order of symbol sizes.

and transitions between them. A crossover from spherical to non-spherical aggregates occurs as the particle size increases for a weak NP–surface interaction strength. The spherical aggregates are disordered. However, the non-spherical aggregates are ordered where particles align face-to-face. As the NP–surface interaction strength increases, clusters of NPs grow uniformly on the surface leading to multilayers of NPs on the surface. Above a certain critical values of the NP–surface interaction strength, only

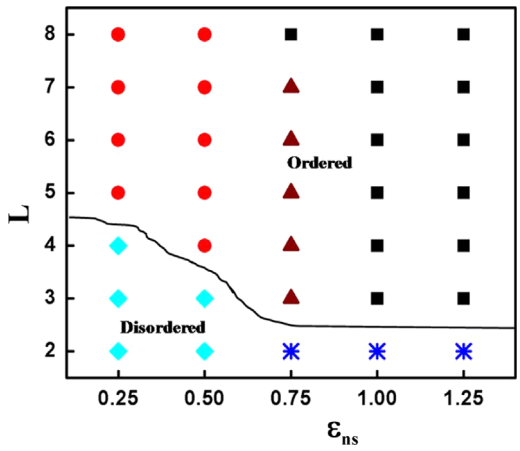

Fig. 11. The phase diagram of triangular NPs in the $L-\varepsilon_{ns}$ plane. ■: Ordered monolayer, ●: aggregates of ordered vertical and horizontal stacks, ▲: ordered multilayer, ◆: 3D disordered aggregate, *: 2D disordered structure. The line is not the thermodynamic boundary. It serves as a guide to eyes.

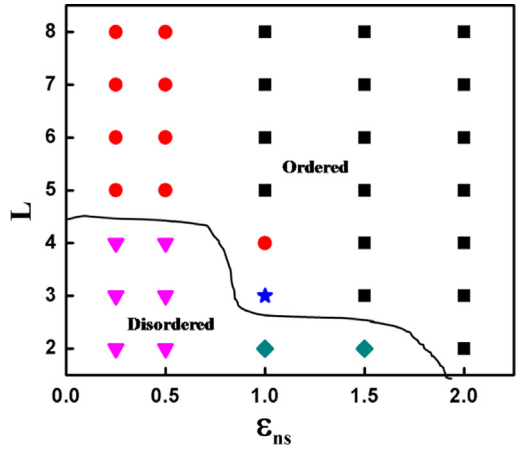

Fig. 12. The phase diagram of tetrahedral NPs in the $L-\varepsilon_{ns}$ plane. ■: Ordered monolayer, ●: non-spherical ordered aggregate, ▼: spherical disordered aggregates, ◆: 2D disordered structure, *: 2D ordered bilayer. The line is to guide eyes, and not a thermodynamics boundary.

monolayers on the surface are formed. In the monolayers, particles are aligned edge-to-edge. The transition from a face-to-face to an edge-to-edge alignment of NPs is dominated by the surface–NP interaction energy. However, the transition from a spherical to a non-spherical aggregate is dominated by the NP–NP interaction energy. We have estimated the phase diagrams that represent all possible structural arrangements of NPs depending on their size and the NP–surface interaction strength. The growth of the cluster depends on the shape and size of particles for low NP–surface interaction strength. The work demonstrates a disorder to order transition as the particle size and the NP–surface interaction strength increases. Thus, the present work delineates the important factors that govern the self-assembly of anisotropic particles on a flat surface.

Acknowledgements

This work is supported by the Department of Science and Technology (DST), Government of India. The computational resources are provided by the Centre for Development and Advance Computing

(CDAC) Pune, India, and the HPC cluster of the Computer Center (CC), Indian Institute of Technology Kanpur. T.K.P acknowledges the Council of Scientific and Industrial Research (CSIR), Government of India, for a senior research fellowship (SRF).

References

Ahmadi, T.S., et al., 1996. Science 272, 1924.
Arciniegas, M.P., et al., 2014. Nano Lett. 14, 1056.
Arkhipov, A., Freddolino, P.L., Schulten, K., 2006. Structure 14, 1767.
Baker, J., Kudrolli, A., 2010. Phys. Rev. E: Stat. Nonlinear Soft Matter Phys. 82, 061304.
Bishop, K.J.M., et al., 2009. Small 5, 1600.
Camargo, P.H.C., et al., 2010. Chem. Phys. Lett. 484, 304.
Chan, G.H., et al., 2008. J. Phys. Chem. C 112, 13958.
Damasceno, P.F., Engel, M., Glotzer, S.C., 2012. Science 337, 453.
Dasgupta, S., Auth, T., Gompper, G., 2014. Nano Lett. 14, 687.
Duan, X., et al., 2001. Nature 409, 66.
Ghezelbash, A., Sigman, M.B., Korgel, B.A., 2004. Nano Lett. 4, 537.
Glotzer, S.C., 2004. Science 306, 419.
Glotzer, S.C., Solomon, M.J., 2007. Nat. Mater. 6, 557.
Graaf, J.d., Roij, R.v., Dijkstra, M., 2011. Phys. Rev. Lett 107, 155501.
Greyson, E.C., Barton, J.E., Odom, T.W., 2006. Small 2, 368.
Grzelczak, M., et al., 2010. ACS Nano 4, 3591.
Haji-Akbari, A., et al., 2009. Nature 462, 773.
Hayton, J.A., Pauliac-Vaujour, E., Moriartyy, P., 2007. Nano 2, 361.
Henzie, J., et al., 2012. Nat. Mater. 11, 131.
Kasture, M., Sastry, M., Prasad, B.L.V., 2010. Chem. Phys. Lett. 484, 271.
Kim, F., et al., 2004. Angew. Chem. Int. Ed. 43, 3673.
Kinge, S., Crego-Calama, M., Reinhoudt, D.N., 2008. ChemPhysChem 9, 20.
Li, F., Josephson, D.P., Stein, A., 2011. Angew. Chem. Int. Ed. 50, 360.
Loudet, J.C., et al., 2005. Phys. Rev. Lett. 94, 018301.
Miller, T.F., et al., 2002. J. Chem. Phys. 116, 8649.
Millstone, J.E., et al., 2009. Small 5, 646.
Min, Y., et al., 2008. Nat. Mater. 7, 527.
Ming, T., et al., 2008. Angew. Chem. Int. Ed. 47, 9685.
Mu, Q., et al., 2012. J. Colloid Interface Sci. 365, 308.
Patra, T.K., Singh, J.K., 2013. J. Chem. Phys. 138, 144901.
Patra, T.K., Singh, J.K., 2014. Soft Matter 10, 1823.
Plimpton, S.J., 1995. J. Comput. Phys. 117, 1.
Radha, B., Kulkarni, G.U., 2011. Cryst. Growth Des. 11, 320.
Rycenga, M., McLellan, J.M., Xia, Y., 2008. Adv. Mater 20, 2416.
Seo, D., et al., 2008. J. Phys. Chem. C 112, 2469.
Seo, Y.S., et al., 2004. Nano Lett. 4, 659.
Smith, B.D., et al., 2014. ACS Nano 8, 657.
Stam, W.v.d., et al., 2014. Nano Lett. 14, 1032.
Tang, Z., et al., 2006. Science 314, 274.
Wang, J.X., et al., 2007. J. Phys. Chem. C 111, 7671.
Wanga, X., et al., 2010. Electrochem. Comm 12, 509.
Xiea, C., et al., 2011. Proc. Natl. Acad. Sci. U.S.A. 108, 15589.
Yamamuro, S., Sumiyama, K., Kamiyama, T., 2008. App. Phys. Lett. 92, 113108.
Yue, T., et al., 2013. Nanoscale 5, 9888.
Zhang, Z., Glotzer, S.C., 2004. Nano Lett. 4, 1407.
Zhang, Z., et al., 2003. Nano Lett. 3, 1341.